Int. Journal of Refractory Metals and Hard Materials 54 (2016) 309–314

Contents lists available at ScienceDirect

Int. Journal of Refractory Metals and Hard Materials

journal homepage: www.elsevier.com/locate/IJRMHM

The effect of phosphorus and nitrogen co-doped on the synthesis of diamond at high pressure and high temperature

Bingmin Yan [a,b], Xiaopeng Jia [a], Chao Fang [a], Ning Chen [a], Yadong Li [a], Shishuai Sun [c], Hong-An Ma [a,*]

[a] *State Key Laboratory of Superhard Materials, Jilin University, Changchun 130012, China*
[b] *Center for High Pressure Science & Technology Advanced Research, Changchun 130012, China*
[c] *College of Science, Tianjin University of Technology, China*

ARTICLE INFO

Article history:
Received 30 June 2015
Accepted 25 August 2015
Available online 2 September 2015

Keywords:
Carbonyl iron powders
High nitrogen diamonds
P/N co-doped diamonds
Hydrogen

ABSTRACT

The synthesis of phosphorus and nitrogen co-doped diamond is investigated in the NiMnCo–C system by adding P_3N_5 or carbonyl iron powders mixed with phosphorus powders under high pressure and high temperature. Experimental results show that the color distribution in diamond crystals with low concentration of P_3N_5 additive is not uniform. The color becomes deep green with the increase of P_3N_5 additive. The optical images and FTIR spectra reveal that the nitrogen atoms are more easily incorporated via {111} than {100} in the same conditions. In addition, the result of FTIR spectra of synthesized diamond indicates that the hydrogen atoms in the form of sp^3–CH_2– are more likely to enter the diamond lattice in the P/N co-doped system, compared with the single N-doped system. The absorption peak at 3107 cm^{-1} attributed to vibration of H-related point defects (sp^2–CH═CH–) is observed in diamonds, which is often found in natural diamonds. The Raman shifting to lower frequency and FWHM value becoming wider are due to the doping of phosphorus atoms.

1. Introduction

Due to its unique physical, mechanical and electrical properties, the diamond as a promising material has attracted wide research for mechanical and electrical applications. Much of this research reveals that the presence of impurities and defects in diamond can affect its mechanical application such as the morphology, hardness, toughness, etc. For electrical applications, we required the fabrication of low-resistivity n-type and p-type material by doping diamond with donor and acceptor impurities, respectively. However, n-type conduction of diamond is basically more challenging than p-type, which has already been achieved by B-doping [1–4]. In recent years, the researchers have focused on nitrogen, phosphorus and sulfur doping primarily. However, the nitrogen atoms incorporated at substitutional sites in diamond form a deep donor level with activation energy of 1.7 eV [5]. No electrical conduction could be observed at room temperature [6–8]. Theoretical candidates for shallow donors are phosphorus (substitutional) [9–11]. However, phosphorus atoms are difficult to incorporate into the diamond lattice, because its atomic radius is larger than the carbon atom. What is more, the electron mobility of P-doped diamond crystal is low, which makes its application problematic at room temperature. The effect on S-doped diamond is similar with P-doping.

Recently, theoretical studies have indicated that the co-doping might be a universal valence control method to overcome self-compensation in wide-gap and super-wide-gap semiconductors [12]. Experimentally, there was still a lack of investigation on the synthesis of co-doped diamonds. HPHT is a kind of effective method to research the single crystal synthetic diamond [13]. Therefore, it is an interesting work to investigate the synthesis and characterization of diamond crystal co-doped with P and N under HPHT conditions. And we expect to improve the characteristics of diamond crystals by P and N synergistically doped, especially their electrical properties.

In this paper, diamond crystals synergistically doped with P and N are successfully obtained, and the FTIR spectra of synthetic diamond indicated that the hydrogen atoms in the form of sp^3–CH_2– can more easily enter into the diamond lattice in the P/N co-doped system. It will be of help for deep understanding of the genesis of natural diamond.

2. Experiment

The synthetic experiments were carried out in a china-type large volume cubic high-pressure apparatus (CHPA) (SPD-6 × 1200) with sample chamber of 10 mm in diameter. The diamond crystallization was run at pressure of 5.8–6.3 GPa and temperature of 1280–1550 °C. Diamonds were synthesized through both film growth method (FGM) and temperature gradient method (TGM). The sample assemblies for diamond synthesized by HPHT are shown in Fig. 1. Graphite with a purity of 99.9% was used as a source of carbon. The synthesized diamond

---

* Corresponding author.
E-mail address: maha@jlu.edu.cn (H.-A. Ma).

http://dx.doi.org/10.1016/j.ijrmhm.2015.08.009
0263-4368/© 2015 Elsevier Ltd. All rights reserved.

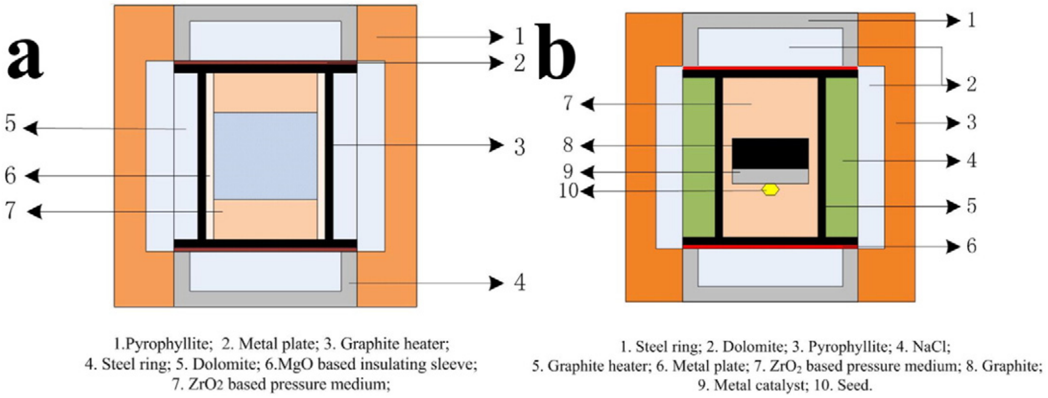

Fig. 1. Sample assembly for diamond synthesized by HPHT. (a) The sample assembly for FGM; (b) the sample assembly for TGM.

Table 1
The corresponding experimental parameters of diamond synthesis with P_3N_5 additive at HPHT conditions.

Run	P_3N_5 (wt.%)	Temperature (°C)	Time (h)	Method
N-a	0.1	1350–1450	0.5	FGM
N-b	0.4	1450–1550	0.5	FGM
N-c	0	1280	15	TGM
N-d	0.15	1300	15	TGM
N-e	0.25	1320	15	TGM
N-f	0.4	1330	15	TGM

(0.8 mm in size) was selected as seed crystal. A NiMnCo alloy was used as the solvent–catalyst. We took the P_3N_5 powders (99.99%), carbonyl iron powders (the special iron with 99 wt.% in purity and 5-10 μm in size) and phosphorus powders as the nitrogen and phosphorus source, respectively. These carbonyl iron powders were synthesized from carbonyl iron with a purity of 99.999 wt.% deoxidizing by iron powders in a stream of ammonia (NH_3) in a running quartz reactor at 300–400 °C. Then the carbonyl iron powders were deoxidized under hydrogen for 1 h. As a result, the major impurities in the carbonyl iron

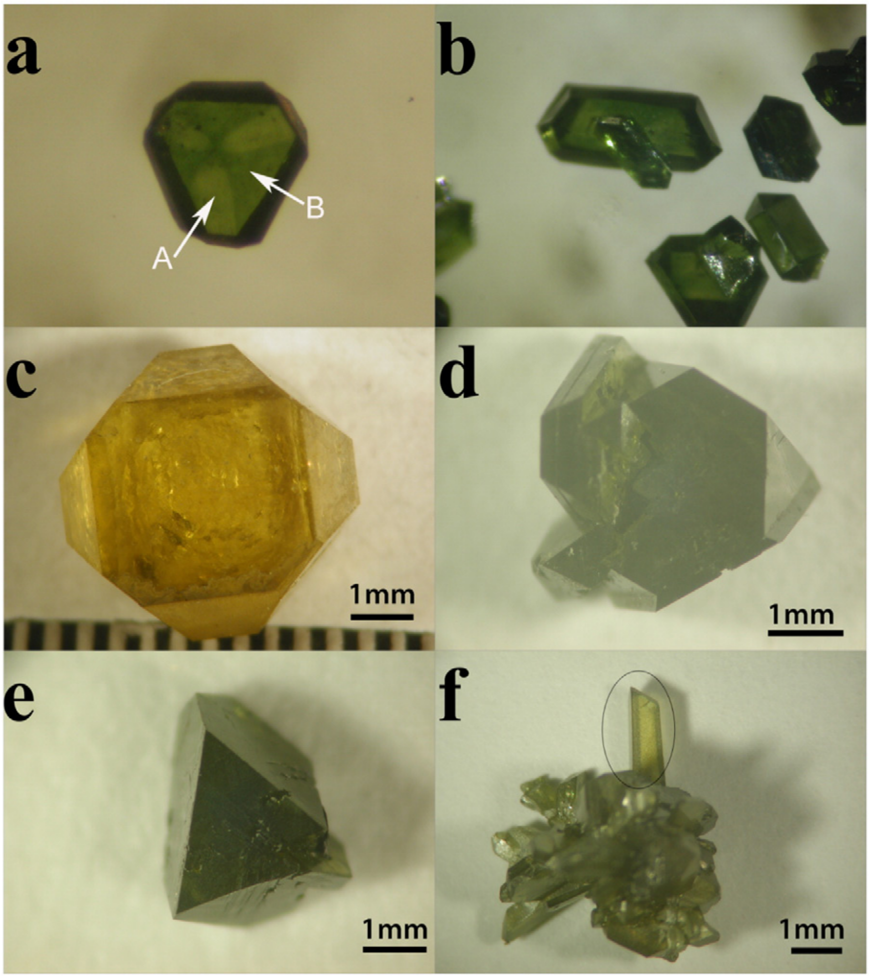

Fig. 2. Optical images of the diamond crystals synthesized from the NiMnCo–C system with P_3N_5 additive: (a) 0.15 wt.%, (b) 0.4 wt.%, (c) 0 wt.%, (d) 0.15 wt.%, (e) 0.20 wt.%, (f) 0.4 wt.%.

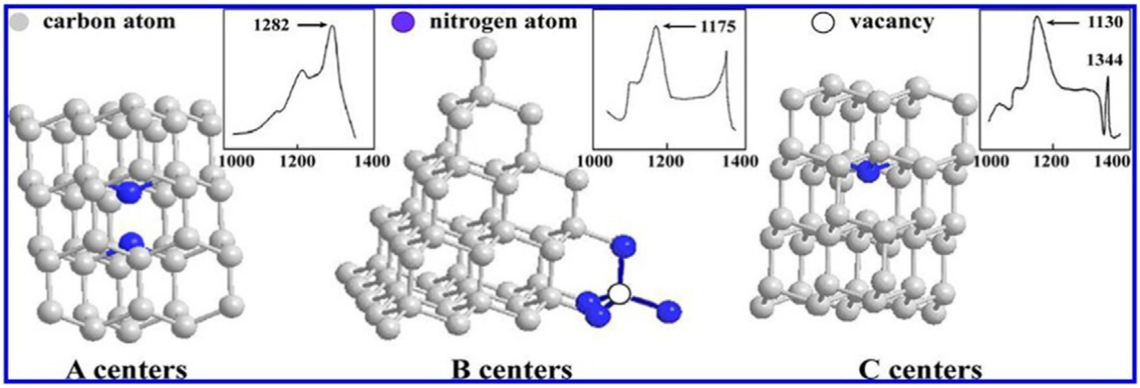

Fig. 3. The schematic drawings of the nitrogen states in diamond and the corresponding typical IR absorption spectra.

powders were N, O, and a little H. The temperature was calibrated using a Pt-30% RH/Pt-6% Rh thermocouple, whose junction was placed near the crystallization sample. Pressure was calibrated at room temperature by the change in resistance of standard substances and at high temperatures by the graphite-diamond equilibrium.

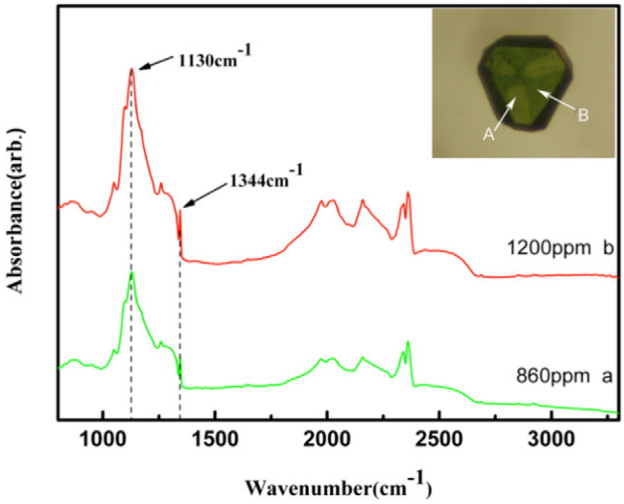

Fig. 4. FTIR spectra of a sample prepared from a octahedral diamond crystals (run N-a). The inset image lying at top right corner is the corresponding optical image of the diamond sample. The spectra of curves (a) and (b) correspond to the A and B zones of diamond.

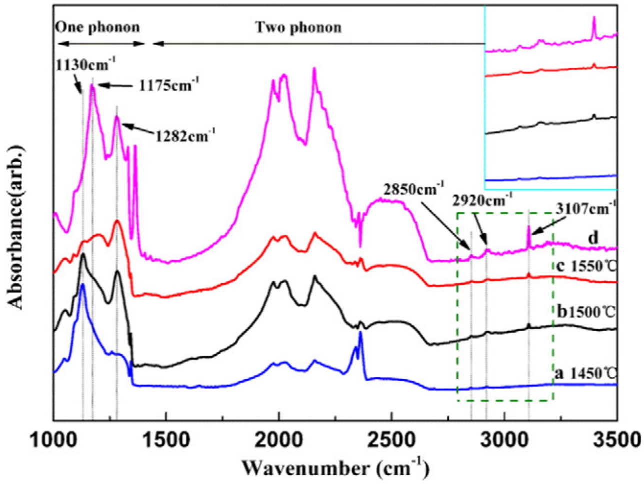

Fig. 5. The typical FTIR recorded for the synthesized diamond crystals by FGM: (a–c) 0.4 wt.% P_3N_5, (d) the natural diamond.

After the HPHT experiment, the samples were placed in a bottle of a boiling mixture of H_2SO_4 and HNO_3 to remove the metal catalysts. The P/N co-doped diamond crystals were characterized by optical microscope. The synthetic diamonds were measured by a Perkin-Elmer 2000 Fourier-transform infrared (FTIR) spectrometer in a spectral range between 400 and 4000 cm^{-1} with a spectral resolution of 2 cm^{-1} in transmittance mode. Furthermore, Raman spectrum and X-ray photoelectron spectroscopy (XPS) were used to confirm their chemical composition and atomic-level hybrid qualities.

3. Results and discussion

3.1. Diamond crystallization and morphology

The diamond crystallization was run in a cubic anvil high pressure and temperature apparatus (SPD-6 × 1200) at temperature of 1280–1550 °C. The main parameters are summarized in Table 1. The diamonds were synthesized at 5.8 GPa (N-a) and 6.0 GPa (N-b) by film growth method (FGM), respectively. The synthesized diamonds exhibit cubic, cub-octahedral and octahedral at 1350–1450 °C, and the color distribution in some diamonds is uneven with 0.1 wt.% (weight ratio in catalyst) P_3N_5 additive (Fig. 2a). The diamonds are light green in some regions and green in other regions. However, when P_3N_5 additive increases to 0.4 wt.%, most of the diamond crystals are deep green in color. More interestingly, some strips are found on the {111} faces (Fig. 2b). In addition to the growth morphology and color, the HPHT conditions on diamond synthesis also change a lot with the increase of P_3N_5 additive.

The experiments (N (c–f)) were run at 6.3 GPa for 15 h by temperature gradient method (TGM). The content of P_3N_5 additive in the catalyst ranges from 0 to 0.4 wt.%. The typical single crystal synthetic diamond without additive displays cubic morphology with developed {100} face, shown in Fig. 2c. At a low concentration of P_3N_5 additive (N-d and e), some slices are found at the intersection of two {100} faces (Fig. 2d and e). However, in experiment (N-f) with 0.4 wt.% P_3N_5 additive, the polycrystalline diamond usually takes initiative as shown in Fig. 2f. From the figure, we can see that the obtained diamond exhibits a green color and displays good octahedral faces. At these conditions,

Table 2
Nitrogen concentrations in diamonds synthesized with 0.4 wt.% P_3N_5 additive.

Sample	Concentration of nitrogen/ppm		
	N_C	N_A	N_{total}
a	1425	0	1425
b	529	202	731
c	371	317	688

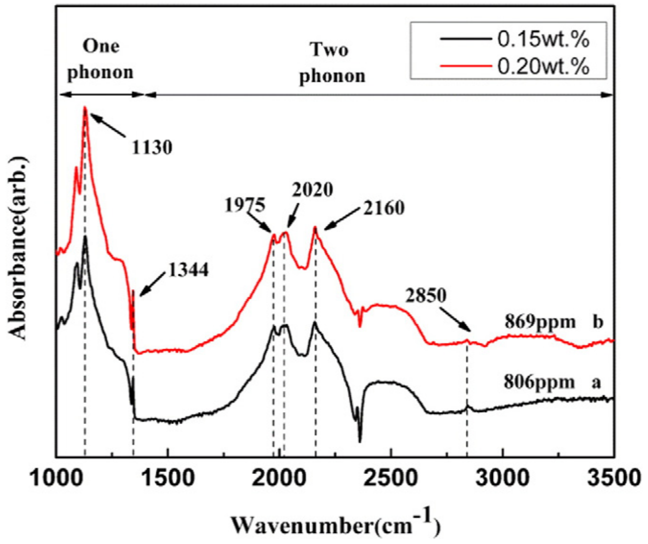

Fig. 6. The typical FTIR recorded for the synthesized diamond crystals by TGM: (a) 0.15 wt.% P_3N_5, (b) 0.20 wt.% P_3N_5.

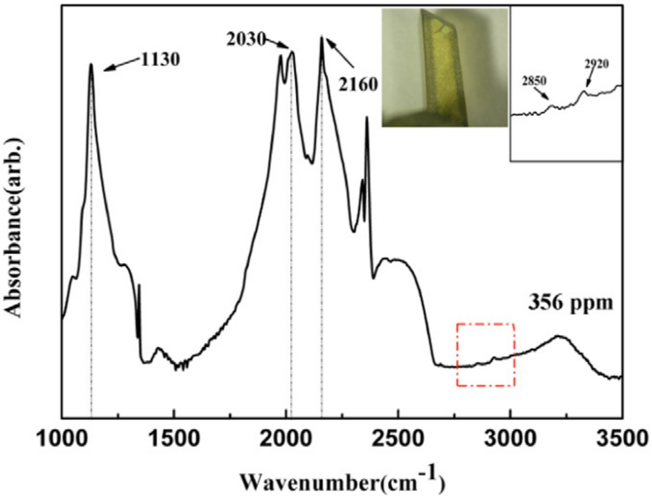

Fig. 7. The typical FTIR recorded for the synthesized diamond crystals with 0.4 wt.% P_3N_5 additive by TGM. The inset image lying at top right corner is the corresponding optical image of the diamond sample. The spectra of curve correspond to the region by circles of diamond in the Fig. 2-f.

the synthesized diamonds are primarily composed of slice and strip shapes. Even so, it is clearly seen that the diamond strips and slices are almost transparent. The transition from single crystal growth to aggregate growth (Fig. 2f) is via the formation of twin crystals (Fig. 2d and e).

3.2. FTIR spectra of the synthesized diamond

The IR absorption is used for quantitative measurements of the nitrogen concentration [14]. Typical FTIR spectra of the synthesized diamond are shown in Fig. 4. All samples show absorption in the defect-induced one-phonon region (1400–800 cm^{-1}) caused by nitrogen impurity. The nitrogen content in the form of A (pairs of nearest neighboring substitutional nitrogen atoms) and C (single substitutional nitrogen atoms) defects are determined by decomposing the IR spectra into A and C components and using the conversion factors of 25 atomic ppm cm^{-1} of absorption at 1130 cm^{-1} for the C defects and 16.5 atomic ppm cm^{-1} of absorption at 1282 cm^{-1} for the A defects. The schematic drawings of the nitrogen states in diamond and the corresponding typical IR absorption spectra are shown in Fig. 3. The nitrogen concentration N_c is given by [15–17]:

$$N_{1130}\,(\mathrm{ppm}) = \mu(1130\ \mathrm{cm}^{-1}) / \mu(2120\ \mathrm{cm}^{-1}) \times 5.5 \times 25$$

$$N_{1282}\,(\mathrm{ppm}) = \mu(1282\ \mathrm{cm}^{-1}) / \mu(2120\ \mathrm{cm}^{-1}) \times 5.5 \times 16.5.$$

Fig. 4 shows the typical FTIR spectra of a diamond crystal with 0.1 wt.% P_3N_5 additive. The sample exhibits two zones. The A region gives light green color, while the B region shows deep green color continuously. The nitrogen concentration of the A and B region are 860 and 1200 ppm, respectively. It proves that the nitrogen atoms are more easily incorporated via {111} compared to {100} in the same conditions.

Fig. 5 shows the FTIR spectra recorded for diamond crystals with 0.4 wt.% P_3N_5 additive and the natural diamond. The concentrations of the nitrogen impurities in the samples (a–c) are summarized in Table 2. Fig. 5 illustrates that nitrogen in diamond is predominantly in the C-form with strong and sharp peaks at 1130 and 1344 cm^{-1} at low temperature (below 1500 °C). At 1500 °C A centers (1282 cm^{-1}) appear and their concentration increases significantly with the increases in temperature. At 1550 °C, we find that the absorption peaks at 1130 and 1344 cm^{-1} for Ib characteristics have almost disappeared, leaving only the stronger absorption peak at 1282 cm^{-1}. It indicates that the synthesized diamond crystal could be classified as the *IaA*-type. The peak intensities of 1282 cm^{-1} reach the maximum with nitrogen concentration of about 317 ppm. In addition to the nitrogen-related bands, the samples also exhibit some absorption peaks related to hydrogen impurity at 2850, 2920 and 3107 cm^{-1}. The absorption peaks at 2850 and 2920 cm^{-1} are responsible for sp^3–CH_2– anti-symmetric vibrations and sp^3–CH_2– symmetric vibrations in diamond, respectively [18–20]. The sharp absorption peak at 3107 cm^{-1} attributed to stretching vibration of hydrogen-related point defects (sp^2–CH═CH–), which is often found in natural diamonds [21–23]. For the synthesized type *IaA* diamond crystals with high nitrogen content mainly in the form of A-center, the absorption peak at 3107 cm^{-1} will be observed [24]. On the basis of previous and present experiments, we can infer that the hydrogen-related infrared absorption has a great correlation with the nitrogen concentration and substitutional form.

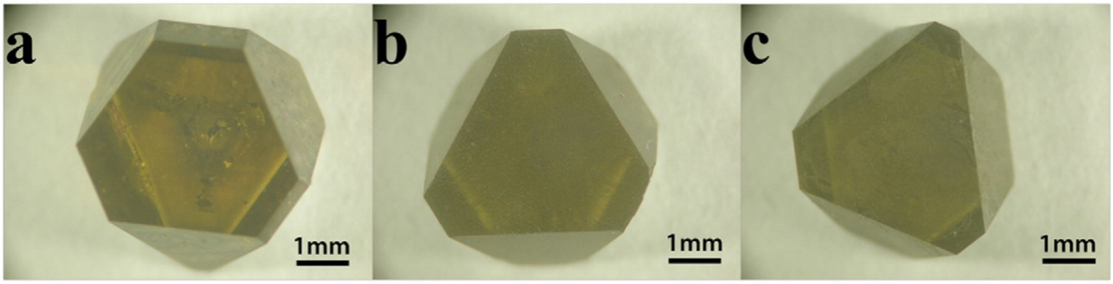

Fig. 8. The optical images of the diamonds obtained from NiMnCo–C system by TGM. (a) 5 wt.% carbonyl iron powders, (b) 5 wt.% carbonyl iron powders + 0.8 wt.% P, (c) 5 wt.% carbonyl iron powders + 1.5 wt.% P.

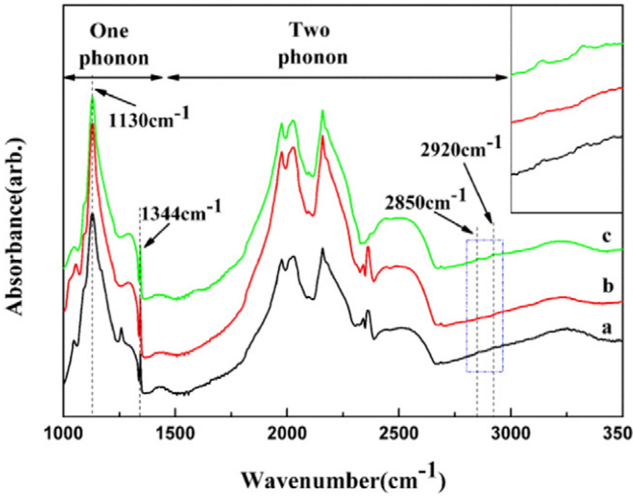

Fig. 9. The typical FTIR recorded for the synthesized diamond crystals: (a) 5 wt.% carbonyl iron powders, (b) 5 wt.% carbonyl iron powders + 0.8 wt.% P, (c) 5 wt.% carbonyl iron powders + 1.5 wt.% P.

The emergence of hydrogen-related absorption peaks is very curious. It should be noted that though hydrogen has been recognized as a common impurity in the natural diamonds, data on its occurrence in the IR spectra form in synthetic HPHT diamonds are very scarce. Kiflawi et al. have found that the 3107 cm^{-1} absorption peak can be produced in some HPHT grown diamonds by annealing at high temperatures [25]. So, we think that the atmosphere sealed in the cavity is more likely the possible hydrogen source in diamond crystallization.

Figs. 6 and 7 show that the optical images and typical FTIR spectra recorded for diamond crystals by TGM with P_3N_5 additive range from 0.15 to 0.4 wt.%. Synthetic crystal is basically polycrystalline diamond. The crystal morphology is very poor with 0.4 wt.% P_3N_5 additive. The nitrogen concentrations are evaluated to be 356–869 ppm. The low nitrogen concentration of Fig. 7 is due to the fast growth for polycrystalline diamond. The hydrogen-related absorption peak at 2850 cm^{-1} has been found. However, we didn't find those hydrogen-related absorption peaks in the FTIR spectra of synthesized diamond with carbonyl iron powders, NaN_3, $Ba(N_3)_2$, and $CaCN_2$, etc. additive. It may indicate that the introduction of phosphorus atoms can promote the hydrogen atoms' entry into the diamond lattice.

In order to verify our speculation, we add some phosphorus powders to the carbonyl iron powder system. Fig. 8 shows optical images of the synthetic diamond crystals. As the phosphorus powder additive increases to 1.5 wt.%, the absorption peaks at 2850 and 2920 cm^{-1} begin to appear (Fig. 9c).

3.3. XPS and Raman measurements

The chemical bonding state of the diamonds is studied by X-ray photoelectron spectroscopy (XPS) measurements. The N 1s, C 1s and P 2p spectra of the samples are shown in Fig. 10, respectively. Fig. 10a shows the N 1s spectrum of the diamond synthesized in our system. It can be deconvoluted into two bands at 399.45 and 400.32 eV, respectively. These bands can be assigned to the graphite-like and pyridine-like N–C structures [26–28]. The deconvolution of the XPS spectrum from the C 1s core level is carried out using XPS singles of C–C, C–N, and C–O bonds, the bonding energies of which are 284.60, 285.69 and 288.60 eV, respectively (Fig. 10b) [26, 29–31]. It is clear that no signal

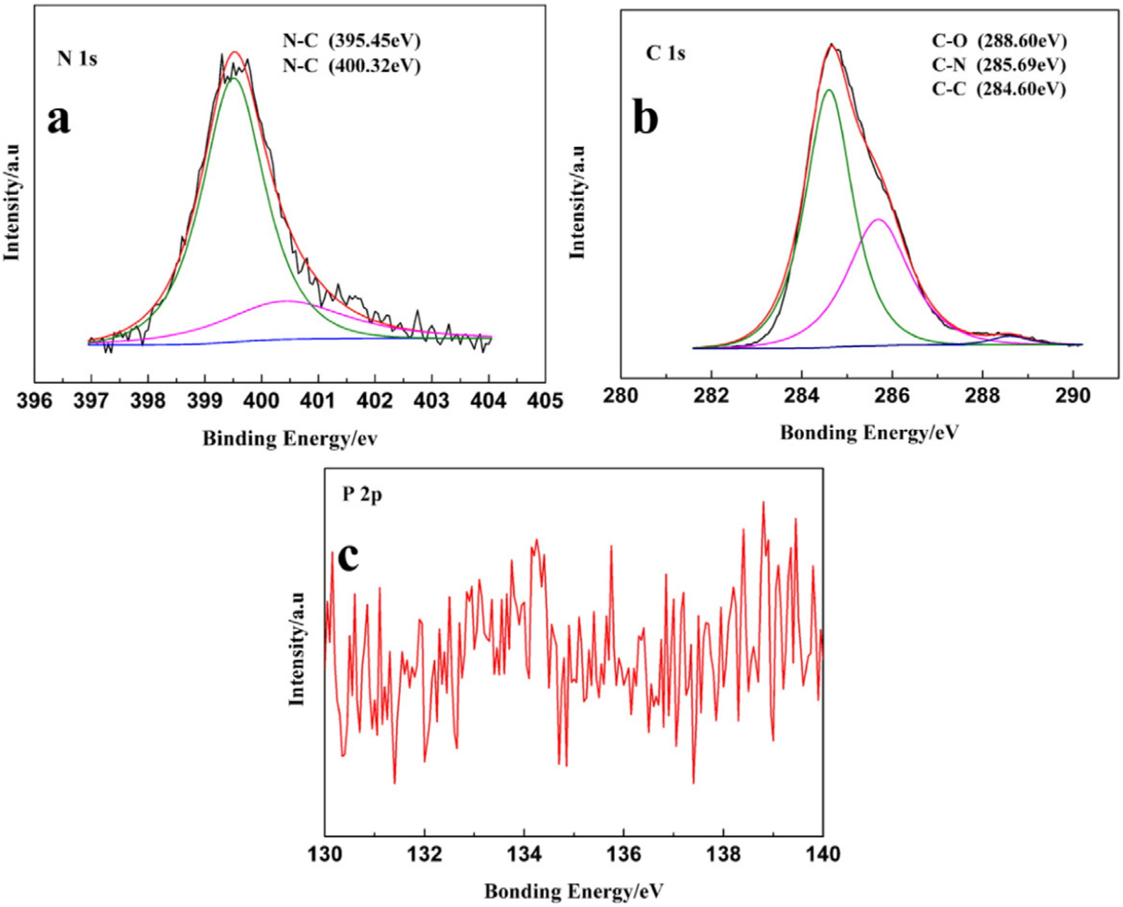

Fig. 10. N s, C 1s and P 2p XPS spectra together with the single Gaussian peak and the deconvolved component peaks for the diamond co-doped with P and N.

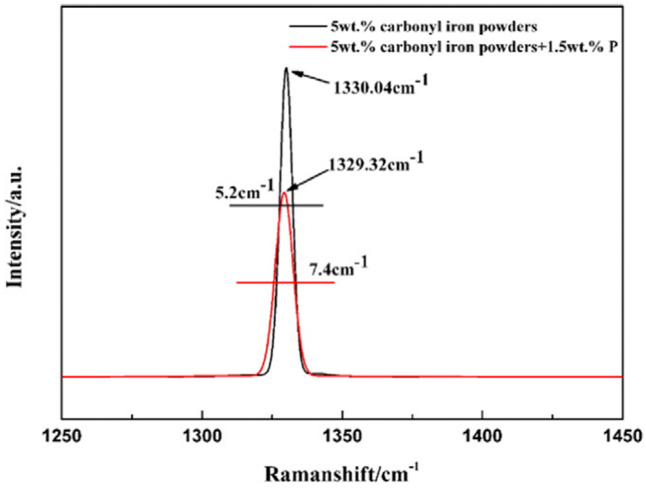

Fig. 11. The Raman peaks and FWHM of the obtained diamonds: (a) 5 wt.% carbonyl iron powders, (b) 5 wt.% carbonyl iron powders + 1.5 wt.% P.

related to P atoms is observed by XPS (Fig. 10c). As we know, the exploration depth of XPS is about 10 nm. Therefore, the XPS measurement may not be the most ideal detection means, because of the low concentration of phosphorus atoms.

To obtain information about the effect of nitrogen and phosphorus atoms on the crystallinity of synthesized diamond crystals, Raman spectra is performed. The Raman spectra of the samples with 5 wt.% carbonyl iron powders and 5 wt.% carbonyl iron powders + 1.5 wt.% phosphorus powder additives are shown in Fig. 11. The Raman peak of diamond with 5 wt.% carbonyl iron powder additive is located at 1330.04 cm^{-1}. It is noticed that the Raman peak of N/P co-doped diamond with 1.5 wt.% P additive is shifted down to 1329.32 cm^{-1}. As is well known, the variation of the full width at half-maximun (FWHM) is usually used to characterize the crystalline order in diamond. We can find that the FWHM value of diamond in the 5 wt.% carbonyl iron powder system is 5.2 cm^{-1}, and the value with 1.5 wt.% P additive is 7.4 cm^{-1}. Previously it has been shown that nitrogen impurity affects the integral perfection of the diamond lattice, giving the rise to defect-induced broadening of the diamond Raman lines. Therefore, we infer that phosphorus atoms enter into the diamond lattices, and make the Raman peaks shift to lower frequency and the FWHM value broaden.

Therefore, one of the reasons for the phenomenon that the introduction of phosphorus atoms can promote the hydrogen atoms' entry into the diamond lattice, may be that the phosphorus atoms caused many defects and formed many carbon atom suspended bonds. As we know, the dissolved nitrogen ability of iron is stronger, and the diamond synthesized in Fe–C system is *IIa* type with low nitrogen concentration. Therefore, we infer that another reason may be the solubility of hydrogen in the catalyst is reduced by phosphorus additive.

4. Conclusion

A series of P and N synergistic doped diamond crystals are successfully synthesized with P_3N_5 and carbonyl iron powders + P additive under pressure 6.3 GPa and temperature ranging from 1280 to 1550 °C. We find that the nitrogen atoms are more easily incorporated via {111} compared to {100} in the same conditions. The FTIR spectra reveal that the hydrogen atoms are more likely to enter the diamond lattice in the P/N co-doped system, compared with the single N-doped system. Hydrogen atoms are mainly incorporated in two forms. The absorption peak at 3107 cm^{-1} attributed to vibration of hydrogen-related point defects (sp^2–CH=CH–) is observed in diamond with A centers. The other is due to sp^3 hybridization C-H bond symmetric (2850 cm^{-1}) and anti-symmetric (2920 cm^{-1}) vibrations. Raman measurement indicates that the phosphorus atoms enter into the diamond lattices. Two possibilities that the phosphorus atoms can promote hydrogen atoms into the diamond lattice are given. And the measurement of the electrical properties of synthetic crystals remains to be further researched.

We believe that our work is helpful for the work on the study of the hydrogen impurity in diamond and the genesis of natural diamond.

Acknowledgments

Project supported by National Natural Science Foundation of China (Grant No. 51172089).

References

[1] S. Koizumi, K. Watanabe, M. Hasegawa, H. Kanda, Science 292 (2001) 1899–1901.
[2] D.C. Shin, B.V. Sarada, D.A. Tryk, A. Fujishima, Anal. Chem. 75 (2003) 530–534.
[3] Y.D. Kim, W. Choi, H. Wakimoto, S. Usami, H. Tomokage, T. Ando, Appl. Phys. Lett. 75 (1999) 3219–3221.
[4] M.H. Latto, D.J. Riley, P.W. May, Diam. Relat. Mater. 9 (2000) 1181–1183.
[5] R.G. Farrer, Solid State Commun. 7 (1969) 685–688.
[6] R. Kalish, Diam. Relat. Mater. 10 (1749–1755) 2001.
[7] A.J. Ecdes, T.A. Steele, A. Afzal, C.A. Rego, W. Ahmed, P.W. May, S.M. Leeds, Thin Solid Films 344/344 (1999) 627–631.
[8] E. Boettger, A. Bluhm, X. Jiang, L. Shafer, C.P. Klages, J. Appl. Phys. 77 (1995) 6332–6337.
[9] S. Koizumi, M. Kamo, Y. Sato, Diam. Relat. Mater. 7 (1998) 540–544.
[10] S.A. Kajihara, A. Antonelli, J. Bernholc, R. Car, Phys. Rev. Lett. 66 (1991) 2010.
[11] K. Jackson, M.R. Pederson, J.G. Harrison, Phys. Rev. B (1990) 41.
[12] T. Nishimatsu, H. Katayama-Yoshida, N. Orita, Mater. Sci. Forum 258–263 (1997) 799–804.
[13] S.S. Sun, X.P. Jia, B.M. Yan, F.B. Wang, N. Chen, Y.D. Li, H.A. Ma, CrystEngComm 16 (2014) 2290–2297.
[14] Y.G. Zou, B.B. Liu, Y.C. Liu, Acta Phys. Sin. 56 (2007) 5172–5175.
[15] I. Kiflawi, A.E. Mayer, P.M. Spear, J.A. VanWyk, G.S. Woods, Philos. Mag. B 69 (1994) 1141–1147.
[16] S.R. Boyd, I. Kiflawi, G.S. Woods, Philos. Mag. B 69 (1994) 1149.
[17] V.I. Bokyj, G.N. Besrukov, Y.N. Kluev, A.M. Naletov, Natural and Synthetic Diamonds, Nauka, Moscow, 1986 219.
[18] P. Coudberg, Y. Catherine, Thin Solid Films 146 (1987) 93–107.
[19] K.M. Mcnamara, B.E. Williams, K.K. Gleason, B.E. Scruggs, J. Appl. Phys. 76 (1994) 2466–2471.
[20] J.E. Field, The Properties of Natural and Synthetic Diamond (London: Academic), 36–411992 81–179.
[21] R.M. Chrenko, R.S. McDonald, K.A. Darrow, Nature 213 (1967) 474–476.
[22] W.A. Runciman, T. Carter, Solid State Commun. 9 (1971) 315–331.
[23] G.S. Woods, A.T. Collins, J. Phys. Chem. Solids 44 (1983) 471–475.
[24] B.M. Yan, X.P. Jia, J.M. Qin, S.S. Sun, Z.X. Zhou, C. Fang, H.A. Ma, Acta Phys. Sin. 63 (2014) 048101.
[25] I. Kiflawi, D. Fisher, H. Kanda, G. Sittas, Diam. Relat. Mater. 5 (1996) 1516–1518.
[26] V. Linss, S.E. Rodil, P. Reinke, M.G. Garnier, P. Oelhafen, U. Kreissig, F. Richter, Thin Solid Films 467 (2004) 76–87.
[27] M.O. Watanabe, S. Itoh, K. Mizushima, T. Sasaki, Appl. Phys. Lett. 68 (1996) 2962–2964.
[28] I. Shimoyama, G. Wu, T. Sekiguchi, Y. Baba, J. Electron Spectrosc. Relat. Phenom. 114–116 (2001) 841–848.
[29] W.J. Pan, J. Sun, H. Ling, N. Xu, Z.F. Ying, J.D. Wu, Appl. Surf. Sci. 218 (2003) 297–304.
[30] C. Morant, P. Prieto, J. Bareno, J.M. Sanz, E. Elizalde, Thin Solid Films 515 (2006) 207–211.
[31] F.L. Huang, C.B. Cao, X. Xiang, R.T. Lv, H.S. Zhu, Diam. Relat. Mater. 13 (2004) 1757–1760.